Horizontal scale study of low-level wind shear based on F-factor

Qi Wang[a], Hong Sun[*a], Kezhi Zhang[b], Qing Wang[b]
[a]CAAC Key Laboratory of Civil Aviation Flight Technology and Flight Safety, Civil Aviation Flight University of China, Guanghan 618300, Sichuan, China; [b]COMAC Shanghai Aircraft Design & Research Institute, Shanghai 201210, China

ABSTRACT

Low-level wind shear is an important weather phenomenon that affects flight safety, and understanding the horizontal scale of low-level wind shear is highly beneficial for wind shear-related research and flight training. Considering the lack of statistics and research in this area in China, this paper proposes a calibration method for the horizontal scale of low-level wind shear based on the F-factor. First, the vertical wind speed is calculated from various flight parameters recorded in the Quick Access Recorder (QAR) data, and then the F-factor is obtained. Second, the wind shear danger period for triggering reactive wind shear warning segments is determined based on the threshold value (±0.105) proposed by the FAA. Third, the horizontal scale of low-level wind shear is estimated by calculating the distance that the aircraft flies during the danger period of the wind shear. Finally, the QAR data from 147 flights triggering reactive wind shear warnings are statistically analyzed, and the mean value of the common horizontal scale of low-altitude wind shear was estimated to be approximately 517 m, with a standard deviation of approximately 135 m.

Keywords: Low-level wind shear, F-factor, QAR, vertical windspeed, horizontal scale

1. INTRODUCTION

Wind shear refers to a phenomenon in which air flow changes dramatically in space and time and is generally defined as low-level wind shear that occurs within 600 m above ground[1,2]. For flights experiencing wind shear, drastic changes in parameters such as the speed, lift and attitude of the aircraft may occur within a short period of time. These issues can pose serious challenges for pilots when performing wind shear procedures, especially since the determination of the end state of a wind shear procedure usually requires pilots to make their own judgments through experience. Therefore, it is highly important to improve pilots' knowledge of wind shear to better accomplish change-out maneuvers, which is of great significance for ensuring aviation safety.

At present, in addition to the pilot's own visual observation, the early warning of wind shear is mainly through the analysis and forecasting of meteorological data by air traffic controllers and the warning information of Doppler weather radar and lidar installed at airports, as well as airborne avionics equipment. To ensure the safety of civil aircraft, various technologies are installed at major airports worldwide[3]. Zhang and others[4-6] studied the characteristics of typical wind shear by radar equipment at different airports around the world, improved the LiDAR wind measurement method, and contributed to optimizing the recognition of low-level wind shear by LiDAR. However, different airports have varying environments, and it is difficult to obtain radar data from different airports. To compensate for the lack of current statistics and research on the horizontal scale of low-level wind shear, in this paper, airborne QAR data is investigated. By analyzing QAR data from flights that triggered reactive wind shear (RWS) warnings, the horizontal scale of wind shear that the aircraft actually crossed was calculated.

Although the calculation principle of the RWS warning parameters in the QAR data has not been published, the occurrence of wind shear can be approximated by the change in the F-factor. The F-factor is an important parameter proposed by FAA for evaluating the strength of wind shear. By calculating the F-factor, the extent of wind shear can be assessed, providing pilots with important flight information to help them make safe flight decisions. The aim of this study is to conduct in-depth research on the horizontal scale of low-level wind shear using airborne QAR data combined with F-factor calculations to help related practitioners, especially pilots, further understand low-altitude wind shear.

*hanksun@263.net

International Conference on Optics, Electronics, and Communication Engineering (OECE 2024), edited by Yang Yue, Proc. of SPIE Vol. 13395, 133952P · © 2024 SPIE · 0277-786X · Published under a Creative Commons Attribution CC-BY 3.0 License · doi: 10.1117/12.3049231

2. F-FACTOR CALCULATION BASED ON THE QAR DATA

2.1 F-factor definition

The F-factor, first introduced in 1990 by RL. Bowles[7] has been widely used for predicting and evaluating wind shear[8-10]. The method is based on the well-established principles of flight mechanics and the current state of knowledge of the phenomenon of wind shear. In essence, via this approach, the total amount of aircraft in the wind shear region is calculated, so that the impact of sudden changes in wind speed on the aircraft can be reflected. This factor is expressed by equation (1) as follows:

$$F = \frac{\dot{W}_x}{g} - \frac{V_{w_z}^e}{V_a} \tag{1}$$

In the above equation, $\dot{W}_x$ is the rate of change in the horizontal wind speed component, $V_{w_z}^e$ is the vertical wind speed component, g is the gravitational acceleration, and V_a is the airspeed. The F-factor indicates the magnitude of the degree to which the aircraft energy is affected by the wind. Specifically, when the F-factor is greater than 0, the wind reduces the energy of the aircraft, which corresponds to the reduction in altitude due to the descending air mass and the loss of airspeed due to the increase in the wind strength; and vice versa.

2.2 Vertical wind speed calculation

The wind speed is an important parameter for evaluating wind shear, and its vector V_w^e can be obtained from the difference between the inertial speed vector V^e and the aerodynamic speed vector V_a^e (where the superscript *e* represents the earth-referenced frame (x, y, z) = (north, east and vertical downward)).

$$V_w^e = V^e - V_a^e \tag{2}$$

where the inertial speed vector V^e is expressed as follows:

$$V^e = \begin{bmatrix} V_x^e \\ V_y^e \\ V_z^e \end{bmatrix}^e = \begin{bmatrix} GS\cos\chi \\ GS\sin\chi \\ -IVV \end{bmatrix}^e \tag{3}$$

Here, V_x^e is the projection of V^e on the x-axis (north), denoted by $GS\cos\chi$; GS is the ground speed; χ is the flight path angle (the angle between the trajectory line and the planned course in flight); V_y^e is the projection of V^e on the y-axis (east), denoted by $GS\sin\chi$; and V_z^e is the projection of V^e on the z-axis (vertical downward) and is expressed by the inertial vertical speed IVV. Since IVV is positive upward, a negative sign is added.

In addition, the aerodynamic speed vector V_a^e can be obtained from V_a^b via coordinate transformation. Here, the superscript b represents the body-referenced frame, with its origin in the center of gravity of the aircraft, the x-axis pointing to the nose along the fuselage, the y-axis pointing to the starboard wing tip, and the z-axis following the right-hand rule vertically downward.

$$\begin{aligned} V_a^e &= [T_{eb}] \cdot V_a^b \\ &= [T_{be}]^{-1} \cdot V_a^b \\ &= [T_{be}]^T \cdot V_a^b \end{aligned} \tag{4}$$

where $[T_{be}]^T$ is the transposition of the transformation matrix converted from the earth-referenced frame (E-frame) to the B-frame (body-referenced frame).

$$[T_{be}]^T = \left[L_1(\phi)L_2(\theta)L_3(\psi)\right]^T = \begin{bmatrix} \cos\theta\cos\psi & -\cos\phi\sin\psi+\sin\phi\sin\theta\cos\psi & \sin\phi\sin\psi+\cos\phi\sin\theta\cos\psi \\ \cos\theta\sin\psi & \cos\phi\cos\psi+\sin\phi\sin\theta\sin\psi & -\sin\phi\cos\psi+\cos\phi\sin\theta\sin\psi \\ -\sin\theta & \sin\phi\cos\theta & \cos\phi\cos\theta \end{bmatrix} \tag{5}$$

$$V_a^b = V_a \cdot \begin{bmatrix} \cos\alpha\cos\beta \\ \sin\beta \\ \sin\alpha\cos\beta \end{bmatrix} \tag{6}$$

where ψ is the yaw angle; θ is the pitch angle, which represents the angle between the x-axis of the B-frame and the horizontal plane; ϕ is the roll angle, which represents the angle between the z-axis of the B-frame and the plumb surface passing through the x-axis of the B-frame; and *a* is the angle of attack, which represents the angle between the chord line of the wing and the vector representing the relative motion between the aircraft and the atmosphere. Since a wing can have twist, the chord line of the whole wing may not be definable, so most commercial jets use the fuselage centerline or longitudinal axis (x-axis) as a reference line. In this paper, *a* is approximated as the angle between the vector representing the relative motion between the aircraft and the atmosphere and the x-axis of the B-frame. β is the sideslip angle, which represents the angle between the direction of the aircraft's relative air motion and the direction of the relative ground motion.

Since the horizontal wind speed component is recorded in the QAR data, this paper focuses on the calculation of the vertical wind speed component. At present, civil aircraft are usually equipped with yaw dampers, which are systems that use sensors, actuators, and controllers to detect and correct yaw. Its controller processes signals such as the yaw rate and sideslip angle and sends commands to the actuator, which moves the rudder to counteract the yaw force on the nose, keeping the aircraft in line with the airflow. Considering that the main function of the yaw damper is to eliminate aircraft sideslip, in this article, it is assumed that the sideslip angles β are 0° in all cases.

Due to the errors in the angle of attack parameters recorded in the QAR data, the acquired angle of attack parameters needs to be corrected. When the aircraft is in straight horizontal flight and is considered to be free of the effects of vertical wind speed, a least square linear fit[11] was chosen for the data from the cruise phase of the aircraft. At this point, the pitch angle θ and roll angle ϕ are small enough to satisfy the small angle approximation condition, so the true angle of attack α_b can be calculated by the simplified equation (7), and then the mean left and right angles of attack recorded in the QAR data can be fitted by equation (8).

$$\alpha_b = \theta - \frac{IVV}{V_a} \tag{7}$$

$$\alpha_b = a_0 + a_1\left(\frac{\alpha_L + \alpha_R}{2}\right) \tag{8}$$

In summary, the component of the wind speed in the z-axis of the E-frame $V_{w_z}^e$ is obtained as follows:

$$V_{w_z}^e = -IVV - V_a \cdot \left(-\sin\theta\cos\alpha_b + \cos\phi\cos\theta\sin\alpha_b\right) \tag{9}$$

3. HORIZONTAL SCALE CALIBRATION OF WIND SHEAR

3.1 Data

In this article, the QAR data of the flight triggered by the RWS, which can record various parameters during the flight, such as true airspeed (TAS), inertial vertical speed (IVV), pitch angle (PITCH), roll angle (ROLL) and angle of attack (AOA), are utilized. Information on the QAR parameters used in the calculations is given in Table 1.

Table 1. QAR parameter meaning and unit.

Name of the QAR data	Meaning	Unit
TAS	True airspeed	kt
GS	Ground speed	kt
WIN_SP	Wind speed	kt
IVV (+=upward)	Inertial vertical speed	ft/min
PITCH (+=nose up)	Pitch angle	degree
ROLL (+=left wing up)	Roll angle	degree
AOAL (+=nose up)	Left vane angle of attack	degree
AOAR (+=nose up)	Right vane angle of attack	degree

3.2 Calculation of the F-factor

In this study, the F-factor calculation is a key step. According to the calculation formula proposed by the FAA, as well as the derivation of the vertical wind speed above, the F-factor can be represented by equation (10). The F-factor can be obtained by providing the corresponding parameters in brackets.

$$F = f\left(TAS, GS, WIN\_SP, IVV, PITCH, ROLL, AOA\right) \tag{10}$$

A large F-factor for only 1 second may represent a gusty disturbance, but consecutively exceeding the threshold is likely to indicate wind shear; therefore, a 5-s continuous F-factor, i.e., the mean $\bar{F}$, is used in this paper as a method of identifying wind shear[1]. $\bar{F}$ is defined by equation (11) as follows:

$$\bar{F}\left(t\right) = \frac{\sum_{t=t_0-5}^{t_0} F\left(t\right)}{5} \tag{11}$$

3.3 Calibration of the horizontal scale of wind shear

This paper defines the hazardous horizontal scale of wind shear as the horizontal extent and size of the area of wind shear that has a large effect on the aircraft such that the aircraft thrust cannot compensate for the loss of airspeed and altitude. In this study, the distance flown by the aircraft is used to approximate the horizontal scale of wind shear. The horizontal scale of wind shear is calculated by determining the wind shear danger period in the RWS event through $\bar{F}$, combined with the ground speed of the aircraft. The specific calculation flow chart is shown in Figure 1.

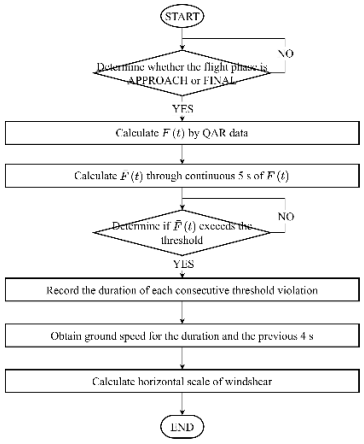

Figure 1. Wind shears horizontal scale calculation process.

Since $\bar{F}$ calculates the average value of the F-factor for a total of 5 s forward from the current moment, a certain amount of time is required to accumulate to reduce false alarms, so there is a certain lag. Therefore, when $\bar{F}$ exceeds the threshold value, the airplane has been in the wind shear region since the first 4 s. In addition, the concatenation of the exceeded threshold time period T_{RWS} and its first 4 s is defined as the wind shear hazard period T_{ws}, which is schematically shown in Figure 2. The formula for calculating the wind shear hazard period T_{ws} is represented by equation (13).

$$T_{RWS} = \left\{ t_i^{RWS} \mid \bar{F}\left(t_i^{RWS}\right) > threshold, i = 1,2,\ldots,n \right\} \tag{12}$$

$$T_{WS} = \left\{ t_1, t_2, \ldots, t_m \right\} = T_{RWS} \bigcup \left\{ t_1^{RWS} - 4, t_1^{RWS} - 3, \ldots, t_1^{RWS} - 1 \right\} \tag{13}$$

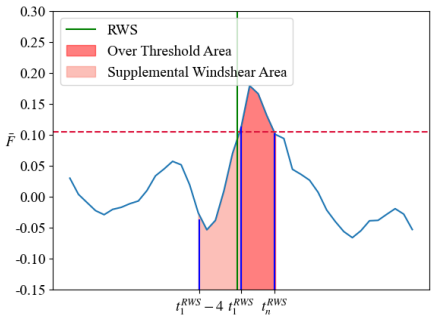

Figure 2. Schematic diagram of the calculation of the horizontal scale of wind shear.

The horizontal scale of wind shear S_{WS} is obtained by integrating the ground speed of the aircraft against time during the wind shear hazard period T_{ws}. QAR data typically behave as discrete data, so it is possible to convert the continuous integral approximation into a discrete summation form. S_{WS} is represented by equation (14):

$$S_{WS} = \sum_{j=1}^{n} \left[GS\left(t_j\right) \cdot \Delta t \right], \left(t_j \in T_{WS}, \Delta t = t_j - t_{j-1} \right) \tag{14}$$

In the above equation, $GS\left(t_j\right)$ is the ground speed at each moment in the wind shear hazard period T_{WS}. Since most of the data in the acquired QAR data are sampled at 1 Hz, Δt in the above equation equals one, and equation (14) can be simplified as follows:

$$S_{WS} = \sum_{j=1}^{n} GS\left(t_j\right), t_j \in T_{WS} \tag{15}$$

4. RESULTS AND DISCUSSION

In this paper, 147 sets of QAR data from flights with RWS triggered were selected, F-factors were calculated, and statistical analyses were performed to derive the common horizontal scale ranges of wind shear, which provide a reference for flight safety. The calculations are analyzed step by step as follows:

4.1 Wind speed calculation results

By analyzing and calculating the QAR data, the variation in the vertical wind speed was obtained. Figure 3 illustrates the horizontal wind speeds recorded in the QAR data and the vertical wind speed variations estimated from the calculations, with the green vertical line representing the RWS warning moment. There are large fluctuations in the horizontal or vertical wind speed before and after triggering the RWS warning, and the fluctuations in the horizontal wind speed are more frequent and stronger than those in the vertical wind speed. This indicates that the RWS is basically horizontal wind shear.

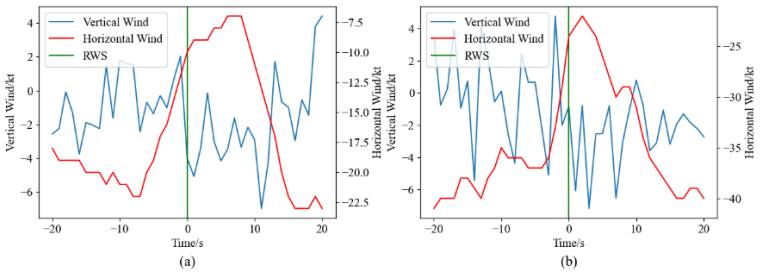

Figure 3. Changes in the horizontal and vertical wind speeds before and after the RWS.

4.2 F-factor analysis

Figure 4 lists the $\bar{F}$ plots of the wind shear for two sets of flights, where the blue curves show the $\bar{F}$ from 20 s before to 20 s after RWS triggering, the green vertical lines represent the moments when the on-board avionics gave RWS as recorded in the QAR data, and the red dashed lines mark the ±0.105 threshold proposed by the FAA. Through comparison, it is found that before and after the RWS warning moments of the on-board avionics' equipment, 65% of the flights in $\bar{F}$ exceed the threshold, while the remaining approximately 35% did not, although the curve has an increasing trend. Thus, this paper mainly focuses on the analysis of the data of the RWS flights that exceeded the threshold.

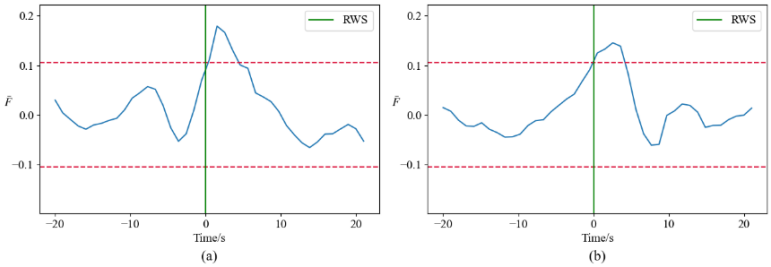

Figure 4. Two sets of wind shear flights $\bar{F}$.

4.3 Statistical analysis of the horizontal scale of wind shear

The statistical analysis of the data of a large number of wind shear events revealed 96 groups of wind shear hazard hours before and after the wind shear event, as shown in Figure 5. The results show that the hazard hours of a large number of wind shear events are concentrated at 7-8 s. The kernel density distribution curves plotted based on the actual data are also closer to the normal distribution curves plotted based on the maximum value of the data, the mean value of the data and the standard deviation of the data. Based on the obtained hazard duration of the wind shear event, combined with the ground speed of the airplane during the wind shear hazard time, the distribution of the wind shear horizontal scale can be approximated, as shown in Figure 6. The results show that 88% of the horizontal scales of low-level wind shear are mainly concentrated between 300 m and 700 m. The mean of the distribution is approximately 517 m, and the standard deviation is approximately 135 m. This result is also closer to the normal distribution, proving that the results are consistent with the statistical law.

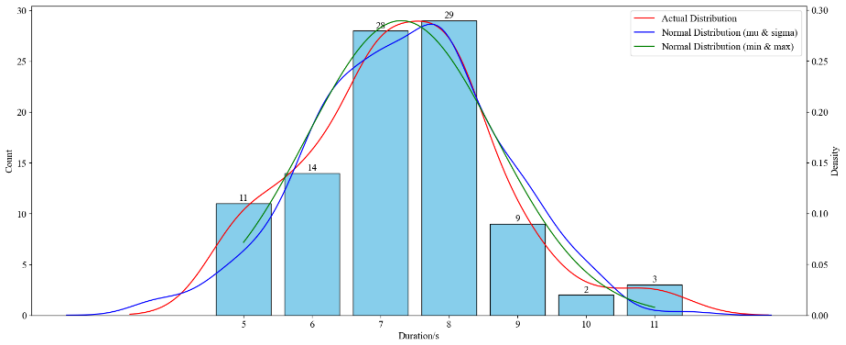

Figure 5. Statistics on the duration of the wind shear hazard period.

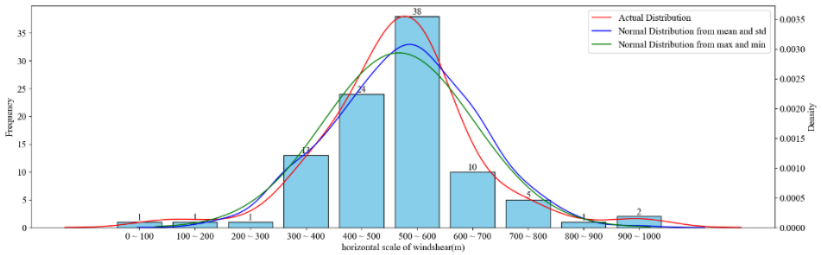

Figure 6. Horizontal scale distribution of the wind shear.

5. CONCLUSIONS AND PROSPECTS

There is currently a lack of industry research on horizontal scales of wind shear. In this study, the feasibility of a method for calculating vertical wind speed was verified using QAR data, and the 5-second mean value of the F-factor $\overline{F}$ in each RWS was calculated from the calculated vertical wind speed and the horizontal wind speed recorded from the QAR data. Finally, the length of the wind shear hazard period in each RWS event was determined, and the horizontal scales of low-level wind shear for a large number of encounters were statistically analyzed in conjunction with the ground speed during the wind shear hazard period. The results of the study provide an important reference for improving the safety of flights. Considering the wide variety of flight parameters recorded by QAR data, future studies can further evaluate the effects of different parameters, optimize the F-factor calculation method based on QAR data, and conduct research on wind field modeling.

ACKNOWLEDGEMENTS

This work was supported in part by the Key Program of Natural Science Foundation of China (Grant No. U2033213), the Fundamental Research Funds for the Central Universities (Grant No. 24CAFUC03009), and the College Students' Innovative Entrepreneurial Training Plan Program (Grant No. S202310624077).

REFERENCES

[1] Lin, C., Zhang, K., Chen, X., Liang, S., Wu, J. and Zhang, W., "Overview of low-level wind shear characteristics over chinese mainland," Atmosphere 12(5), 628 (2021).
[2] International Civil Aviation Organization, "Manual on low-level wind shear (Doc 9995)," <https://store.icao.int/en/manual-on-low-level-wind-shear-and-turbulence-doc-9817> (2005).
[3] Khattak, A., Chan, P. W., Chen, F. and Peng, H., "Prediction of a pilot's invisible foe: The severe low-level wind shear," Atmosphere 14(1), 37 (2023).
[4] Zhang, H., Wu, S., Wang, Q., Liu, B., Yin, B. and Zhai, X., "Airport low-level wind shear lidar observation at Beijing Capital International Airport," Infrared Physics & Technology 96, 113-122 (2019).
[5] Li, L., Shao, A., Zhang, K., Ding, N. and Chan, P.-W., "Low-level wind shear characteristics and lidar-based alerting at Lanzhou Zhongchuan International Airport, China," J. Meteorol. Res. 34(3), 633-645 (2020).
[6] Yuan, J., Su, L., Xia, H., Li, Y., Zhang, M., Zhen, G. and Li, J., "Microburst, windshear, gust front, and vortex detection in Mega Airport using a single coherent doppler wind lidar," Remote Sensing 14(7), 1626 (2022).
[7] Li, F., Xu, X., Li, J., Hu, H., Zhao, M. and Sun, H., "Wind Shear operation-based competency assessment model for civil aviation pilots," Aerospace 11(5), 363 (2024).
[8] Lee, Y. F. and Chan, P. W., "LIDAR-based F-factor for wind shear alerting: Different smoothing algorithms and application to departing flights," Meteorological Applications 21(1), 86-93 (2014).
[9] Chan, P. W., "Application of LIDAR-based F-factor in windshear alerting," METZ 21(2), 193-204 (2012).
[10] Zhao, S., Zhao, W., Shan, Y. and Tian, X., "Research on wind shear identification method based on combined F-factor," Third International Computing Imaging Conference (CITA 2023) 12921, 864-878 (2023).
[11] Sharman, R. D., Cornman, L. B., Meymaris, G., Pearson, J. and Farrar, T., "Description and derived climatologies of automated in situ eddy-dissipation-rate reports of atmospheric turbulence," Journal of Applied Meteorology and Climatology 53(6), 1416-1432 (2014).